DIS2023

East Lansing, Michigan (USA)

28 March 2023

Precision measurements of jet and photon production at ATLAS

Daniel Camarero Muñoz, Brandeis University
On behalf of the ATLAS collaboration
daniel.camarero.munoz@cern.ch

Precision measurements of jet and photon production at ATLAS

- **Measurements of inclusive isolated-photon cross sections provide a testing ground for pQCD with a hard colourless probe**
  - Sensitivity to the gluon density in the proton (via $qg \rightarrow q\gamma$) → input for PDF fits
- **Event shapes are a class of observables defined as functions of the final-state particles four-momenta, which characterise the hadronic energy flow in a collision**
  - The study of these observables in multijet production provides stringent tests of pQCD
- **Focus on three measurements in this talk:**
  - Inclusive-photon production and its dependence on photon isolation in *pp* collisions at $\sqrt{s} = 13\ \mathrm{TeV}$ using $139\ \mathrm{fb}^{-1}$ of ATLAS data [arXiv:2302.00510]
  - Determination of the strong coupling constant from transverse energy-energy correlations in multijet events at $\sqrt{s} = 13\ \mathrm{TeV}$ with the ATLAS detector [arXiv:2301.09351]
  - Measurements of multijet event isotropies using optimal transport with the ATLAS detector [ATLAS-CONF-2022-056]

Precision measurements of jet and photon production at ATLAS

- **Measurements of inclusive isolated-photon cross sections provide a testing ground for pQCD with a hard colourless probe**
  - Sensitivity to the gluon density in the proton (via $qg \to q\gamma$) $\to$ input for QCD fits
- **Event shapes are a class of observables defined as functions of the final-state particles four-momenta, which characterise the hadronic energy flow in a collision**
  - The study of these observables in multijet production provides stringent tests of pQCD
- **Focus on three measurements in this talk:**
  - Inclusive-photon production and its dependence on photon isolation in *pp* collisions at $\sqrt{s} = 13\ \mathrm{TeV}$ using $139\ \mathrm{fb}^{-1}$ of ATLAS data [arXiv:2302.00510]
  - Determination of the strong coupling constant from transverse energy-energy correlations in multijet events at $\sqrt{s} = 13\ \mathrm{TeV}$ with the ATLAS detector [arXiv:2301.09351]
  - Measurements of multijet event isotropies using optimal transport with the ATLAS detector [ATLAS-CONF-2022-056]

Inclusive-photon production: overview

- **The production of high-p_T prompt γ proceeds via two mechanisms**
  (**Prompt photons:** photons not coming from hadron decays)
- **Previous studies performed using $36\ \mathrm{fb}^{-1}$ from the $2015+2016$ datasets**
- **Full Run-2 analysis of inclusive-isolated photon cross sections**
  - $\mathrm{d}\sigma/\mathrm{d}E_T^\gamma$ measured for two γ-isolation cone sizes: $R=0.2$, and $R=0.4$
    - Test the R-dependence of the inclusive photon cross sections at 13 TeV. [**motivation:** JHEP 04 (2020) 166]
  - Fine $|\eta^\gamma|$ regions: [0.0, 0.6, 0.8, 1.37, 1.56, 1.81, 2.01, 2.37]
    - Detailed experimental information for PDF fits
  - Photons with $E_T^\gamma > 250\ \mathrm{GeV}$ and $|\eta^\gamma| < 2.37$ (excluding $1.37 < |\eta^\gamma| < 1.56$)
  - Tight *identification* and *isolation*: $E_{T,\mathrm{cut}}^{\mathrm{iso}} = 4.2\times 10^{-3}\times E_T^\gamma + 4.8\ \mathrm{GeV}$

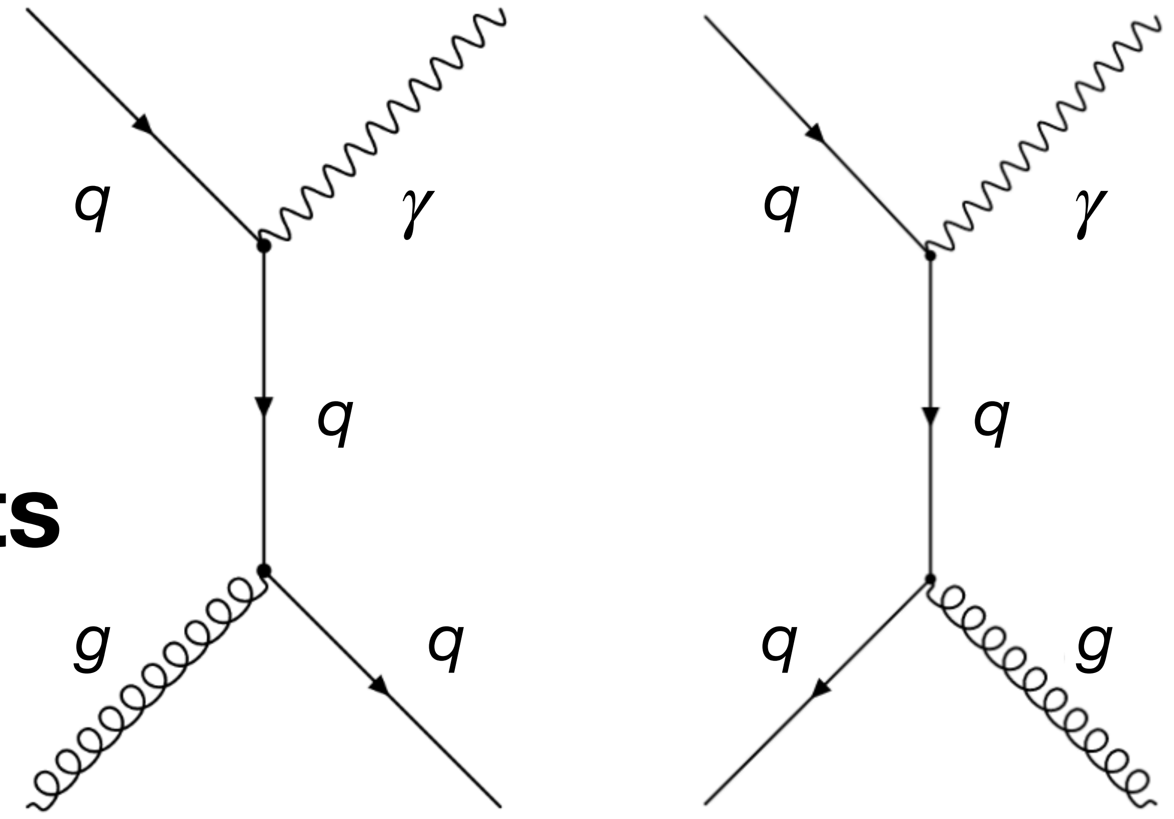

Direct processes

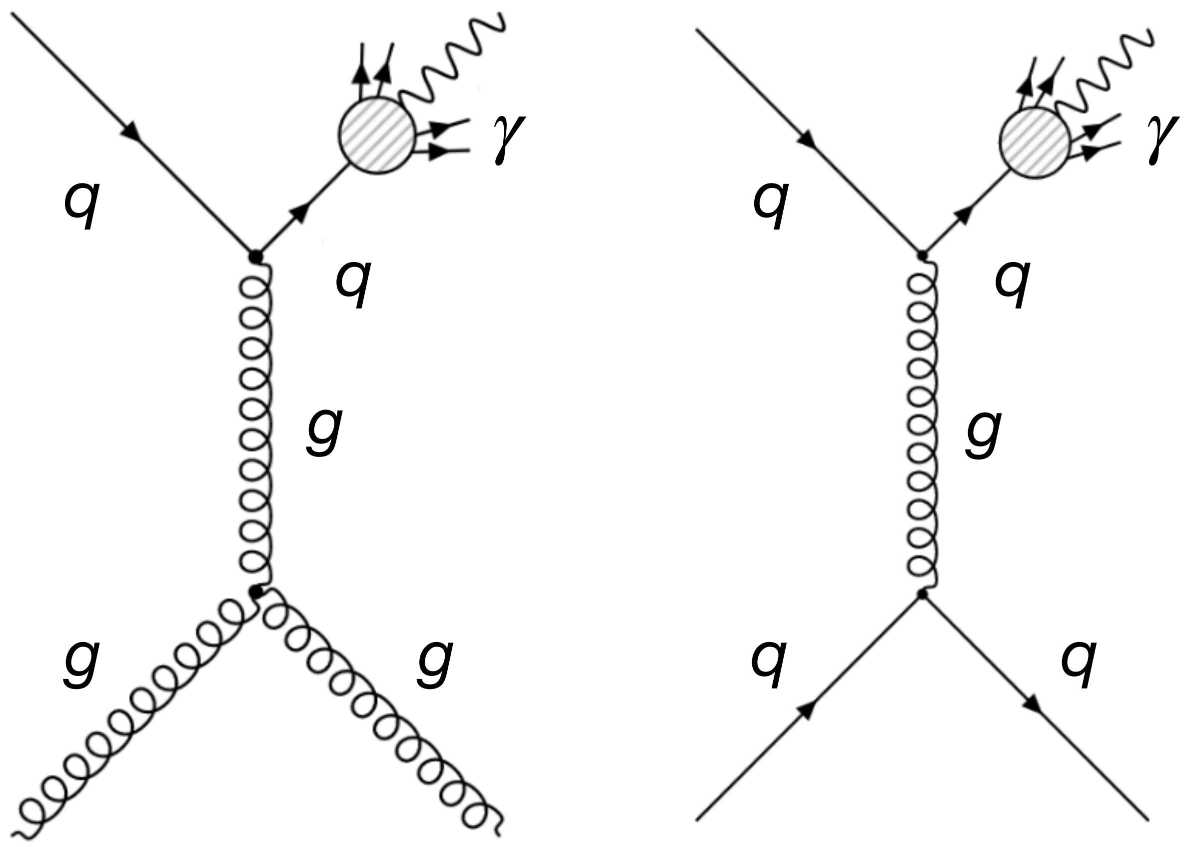

Fragmentation processes

Inclusive-photon production: theoretical predictions

JETPHOX (fixed order)

- **Full fixed-order NLO pQCD calculations for direct and fragmentation processes**
- **Scales:** $\mu_R = \mu_F = \mu_f = E_T^\gamma/2\,(E_T^\gamma)$
- **Fragmentation functions:** BFG II
- **PDFs:** MMHT2014, CT18, NNPDF3.1, and HERAPDF2.0 at NLO; ATLASpdf21 at NNLO
- **Isolation:** fixed cone at parton level
- **Non-perturbative corrections:** estimated using PYTHIA samples. Consistent with unity within $\pm 1\ \%$ (no correction applied)

SHERPA NLO (multileg merged)

- **Parton-level calculations for $\gamma + 1{,}2\,(3{,}4)$ jets at NLO (LO) supplemented with PS**
- Only direct contribution (Frixione's isolation at ME level)
- **Scales:** dynamic scale setting (E_T^γ)
- **PDFs:** NNPDF3.0 NNLO
- **Fragmentation into hadrons and UE simulated as for SHERPA LO**
- **Isolation:** fixed cone at particle level

NNLOJET (fixed order)

- **Full fixed-order NNLO pQCD calculations for direct and fragmentation processes**
- **Scales:** $\mu_R = \mu_F = E_T^\gamma$

$$\mu_f = \sqrt{E_T^\gamma \cdot E_T^{\max}} \cdot R$$

- **Fragmentation functions:** BFG II
- **PDFs:** CT18 NNLO
- **Isolation:** fixed cone at parton level
- **Non-perturbative corrections:** same estimation as for JETPHOX

- **Theoretical uncertainties:** scale variations (scales $\times\, 0.5$ or $\times\, 2$ varied singly or simultaneously), PDFs, α_S, and non-perturbative corrections (only for JETPHOX & NNLOJET)
- NNLO scale uncertainties reduced by more than a factor 2 compared to those of NLO JETPHOX and SHERPA calculations

Inclusive-photon production: differential cross sections

- Measured cross sections compared to the NLO QCD predictions of JETPHOX as a function of E_T^γ in the different $|\eta^\gamma|$ regions
  - **Several PDFs compared:** MMHT2014, CT18, NNPDF3.1, HERAPDF2.0, and ATLASpdf21

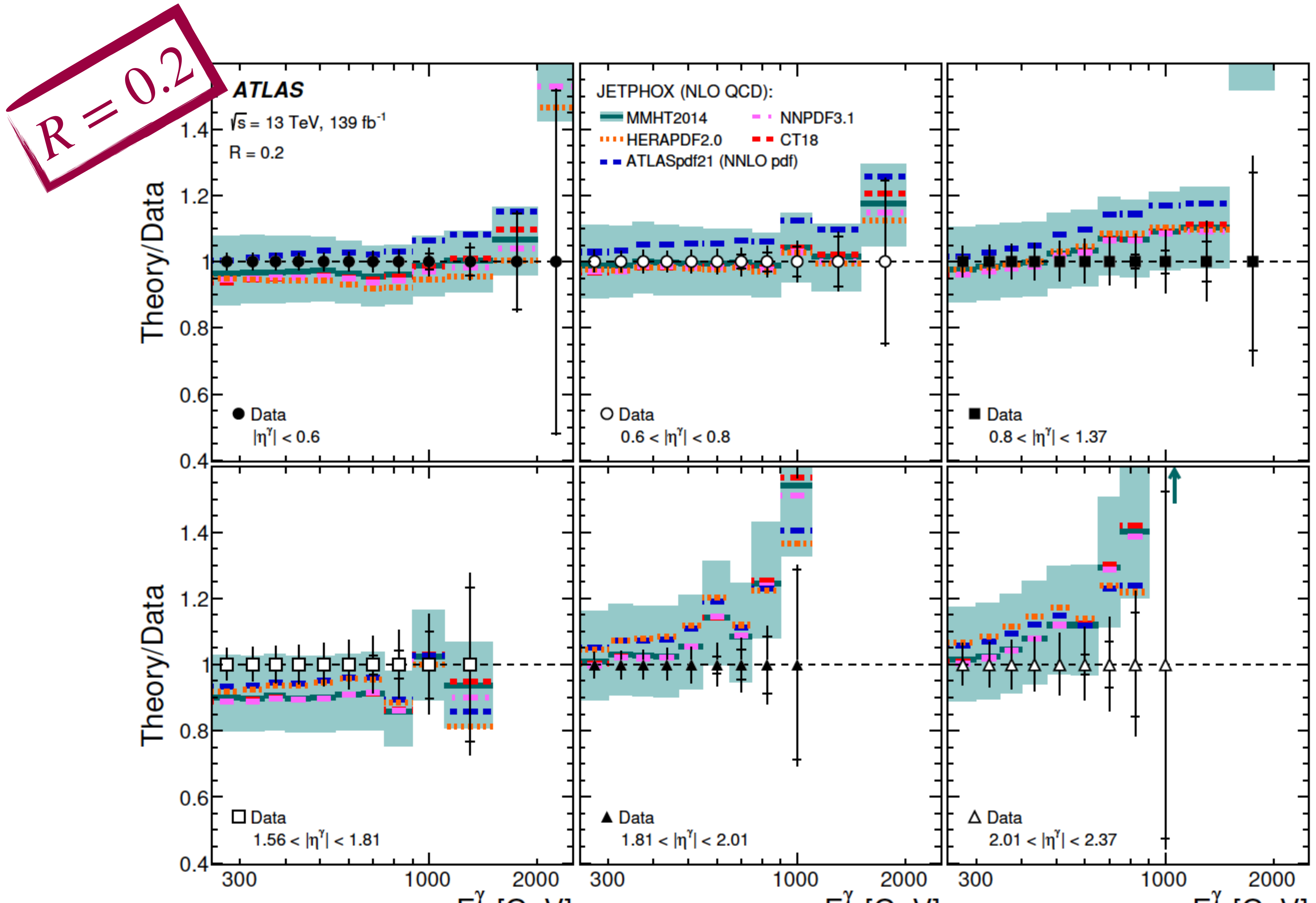

(a)

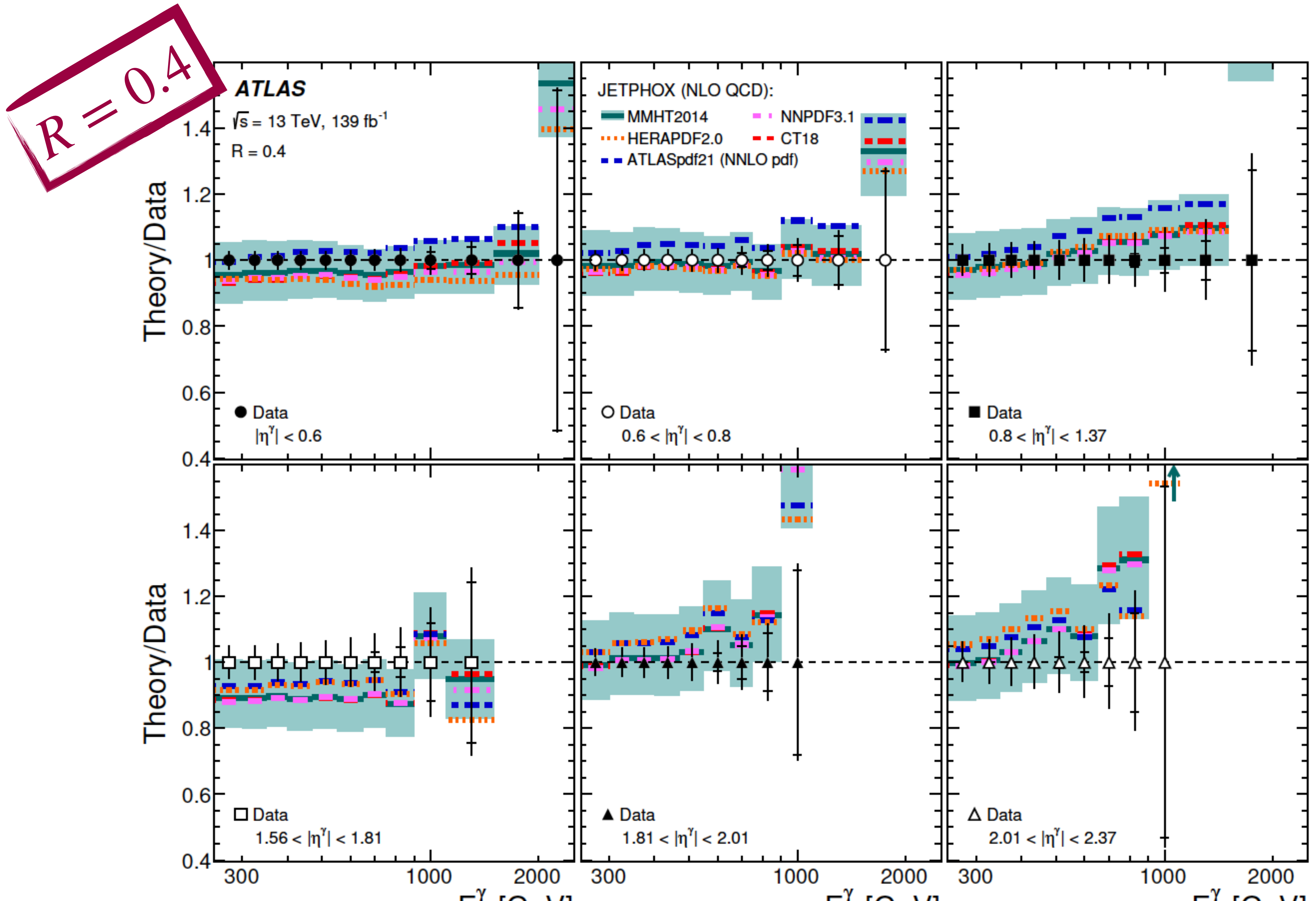

(b)

arXiv:2302.00510

- **Systematic uncertainties** dominated by the photon energy scale, luminosity, pile-up and R^{bg} correlation. Total uncertainty in the range $3\% - 20\,\%$, depending on the E_T^γ and $|\eta^\gamma|$ region.

Inclusive-photon production: ratios of differential cross sections

arXiv:2302.00510

- The dependence on R of the cross sections is studied by measuring the ratios of the differential cross sections for $R = 0.2$ and $R = 0.4$ as functions of E_T^γ in the different $|\eta^\gamma|$ regions

- **These measurements provide a very stringent test of pQCD with reduced experimental and theoretical uncertainties (both $\sim 1\%$!)**
    - Validation of the underlying pQCD theoretical description up to $\mathcal{O}(\alpha_S^2)$

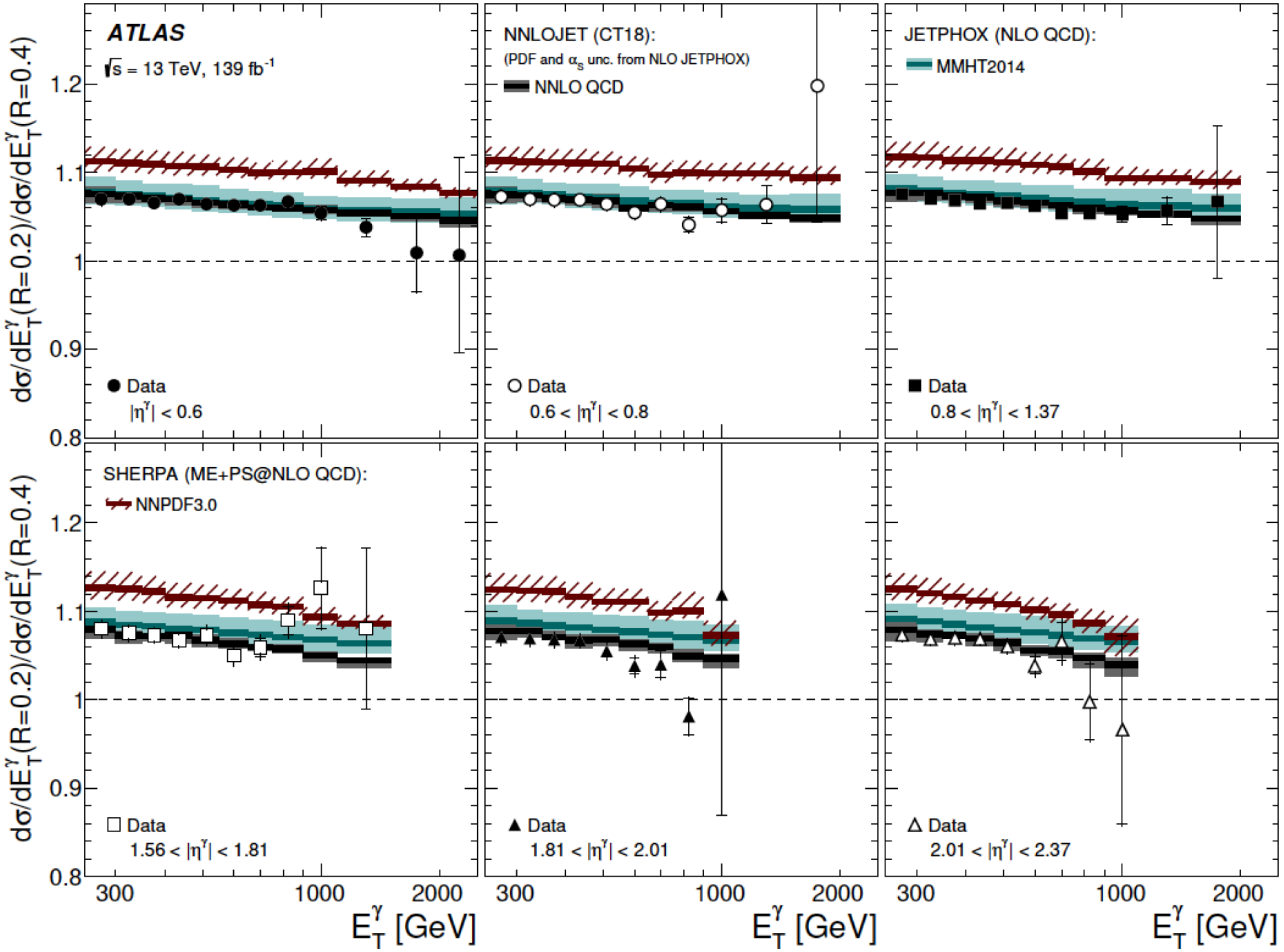

Transverse energy-energy correlations: overview

- **TEEC function:** transverse energy-weighted distribution of the azimuthal differences between jet pairs in the final state

$$\frac{1}{\sigma}\frac{\mathrm{d}\Sigma}{\mathrm{d}\cos\phi} = \frac{1}{N}\sum_{A=1}^{N}\sum_{ij}\frac{E_{\mathrm{T}i}^{A}E_{\mathrm{T}j}^{A}}{\left(\sum_k E_{\mathrm{T}k}^{A}\right)^2}\delta\left(\cos\phi - \cos\varphi_{ij}\right)$$

- **ATEEC function:** difference between the forward ($\cos\phi > 0$) and backward ($\cos\phi < 0$) parts of the TEEC function

$$\frac{1}{\sigma}\frac{\mathrm{d}\Sigma^{\mathrm{asym}}}{\mathrm{d}\cos\phi} = \frac{1}{\sigma}\frac{\mathrm{d}\Sigma}{\mathrm{d}\cos\phi}\bigg|_{\phi} - \frac{1}{\sigma}\frac{\mathrm{d}\Sigma}{\mathrm{d}\cos\phi}\bigg|_{\pi-\phi}$$

  - **Large sensitivity to QCD radiation and the strong coupling constant $\alpha_{\mathrm{S}}(Q)$**
  - **Mild sensitivity to PDFs and factorisation and renormalisation scale variations**

- **Full Run-2 analysis performed using $139\ \mathrm{fb}^{-1}$**
  - Jet selection: $p_{\mathrm{T}} > 60\ \mathrm{GeV}$ and $|\eta| < 2.4$
  - Event selection: $N_{\mathrm{jet}} \geq 2$ and $H_{\mathrm{T2}} = p_{\mathrm{T1}} + p_{\mathrm{T2}} > 1\ \mathrm{TeV}$
  - Ten bins of H_{T2} in which the TEEC and ATEEC are measured: [1000,1200,1400,1600,1800,2000,2300,2600,3000,3500,∞]

Transverse energy-energy correlations: measured observables

- Measured cross section compared to the MC predictions of PYTHIA, SHERPA and HERWIG, for the TEEC (left) and ATEEC (right) distributions in the inclusive H_{T2} bin

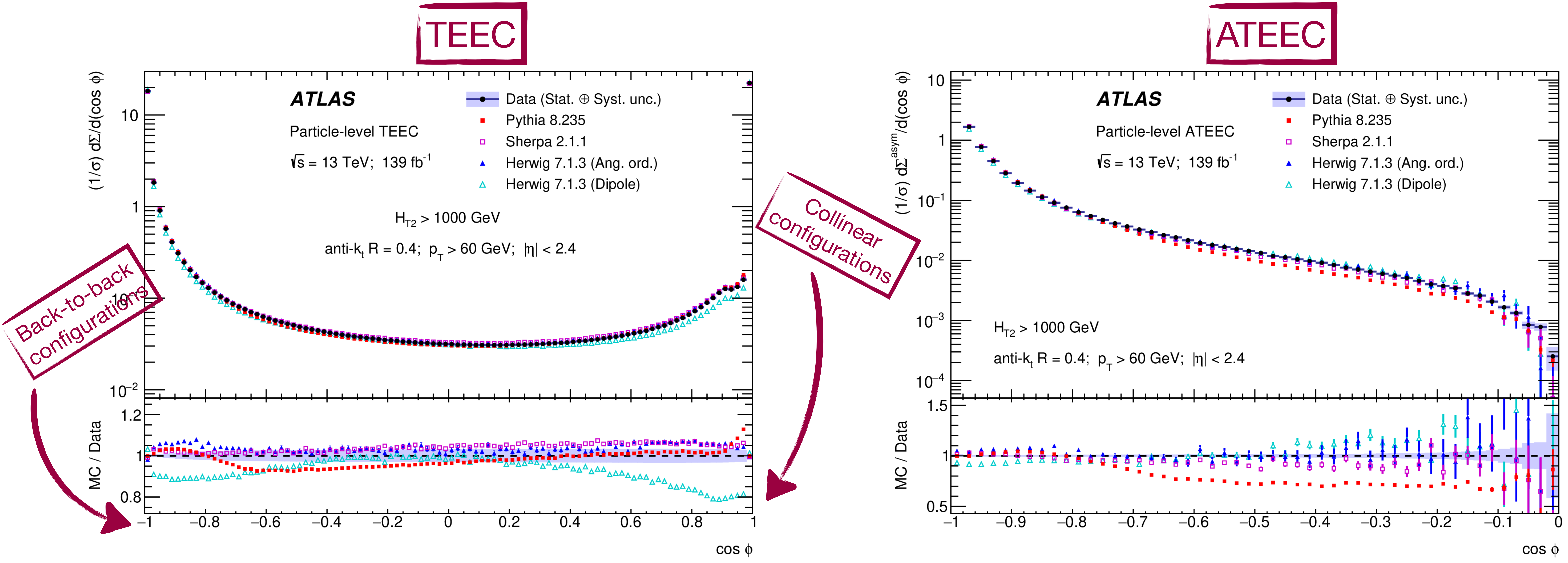

arXiv:2301.09351

- **Systematic uncertainties** dominated by that in the jet energy scale and the Monte Carlo model used to correct for detector effects. Total uncertainty of order $2\,\%$ $(1\,\%)$ for the TEEC (ATEEC).

Transverse energy-energy correlations: theoretical predictions

- Full fixed-order NNLO theoretical predictions for 3-jet cross sections obtained by M. Czakon, A. Mitov and R. Poncelet [Phys. Rev. Lett. 127 (2021) 152001, arXiv:2301.01086]

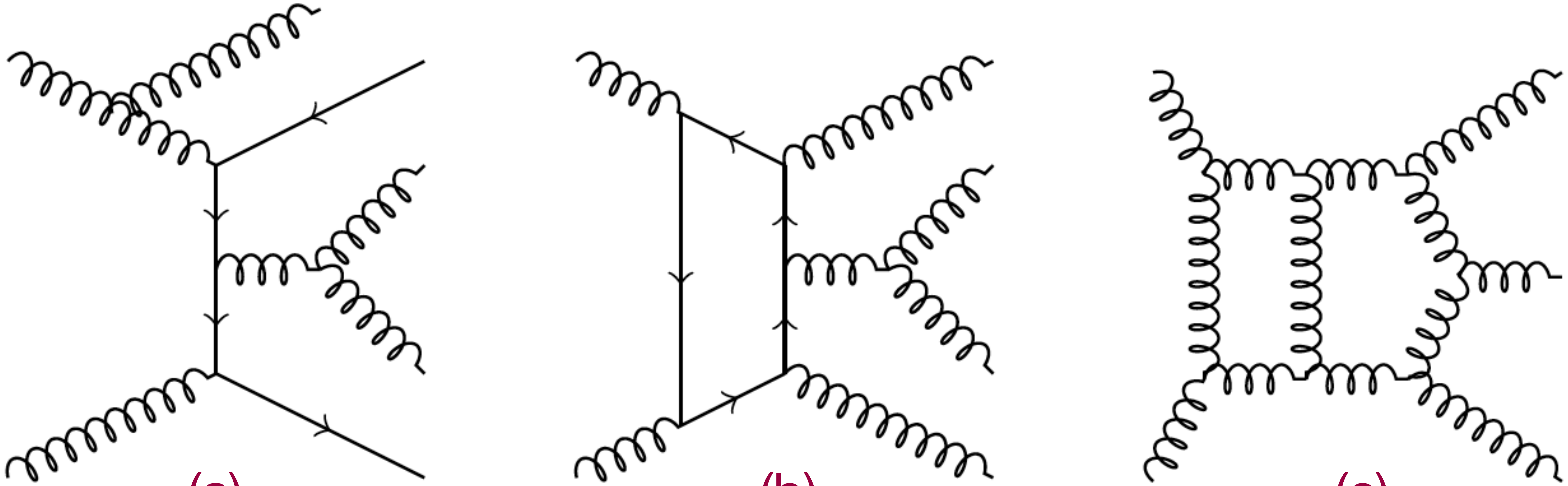

arXiv:2301.09351

- NNLO corrections calculated using $\mathcal{O}(10^{13})$ events, including real-real (a), virtual-real (b), and virtual-virtual (c) finite terms
  - Renormalisation and factorisation scales: $\mu_R = \mu_F = \hat{H}_{\mathrm{T}}$ (scalar sum of p_{T} of all final-state partons)
  - Non-perturbative corrections estimated using PYTHIA, close to unity within $0.5\ \%$ for most of the phase space
  - **Theoretical uncertainties:** scale variations, PDFs and non-perturbative corrections uncertainties
    - Reduction by a factor of 3 in both the cross sections for TEEC and ATEEC and in the $\alpha_{\mathrm{S}}(Q)$ determination

Transverse energy-energy correlations: results

TEEC

ATEEC

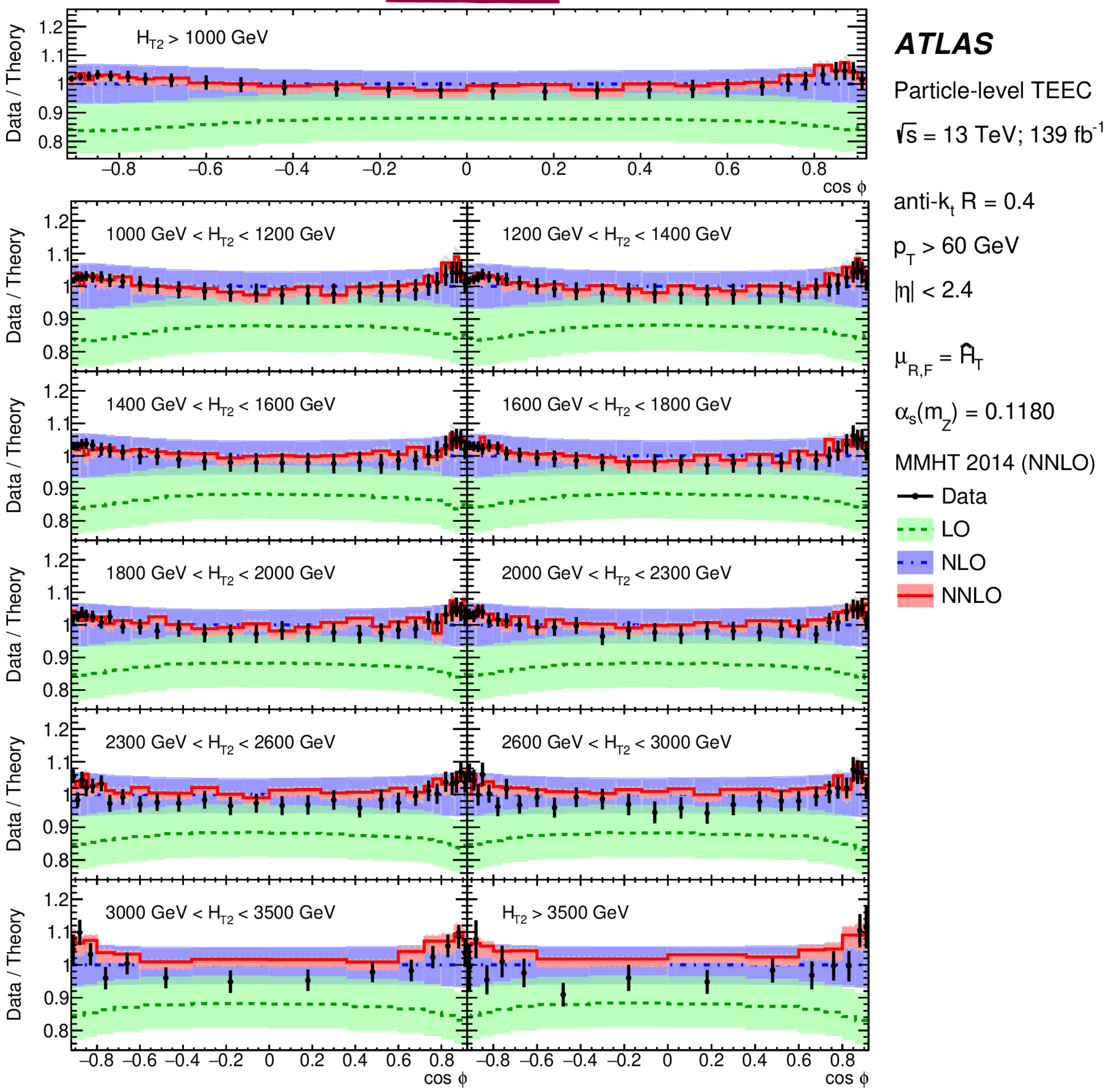

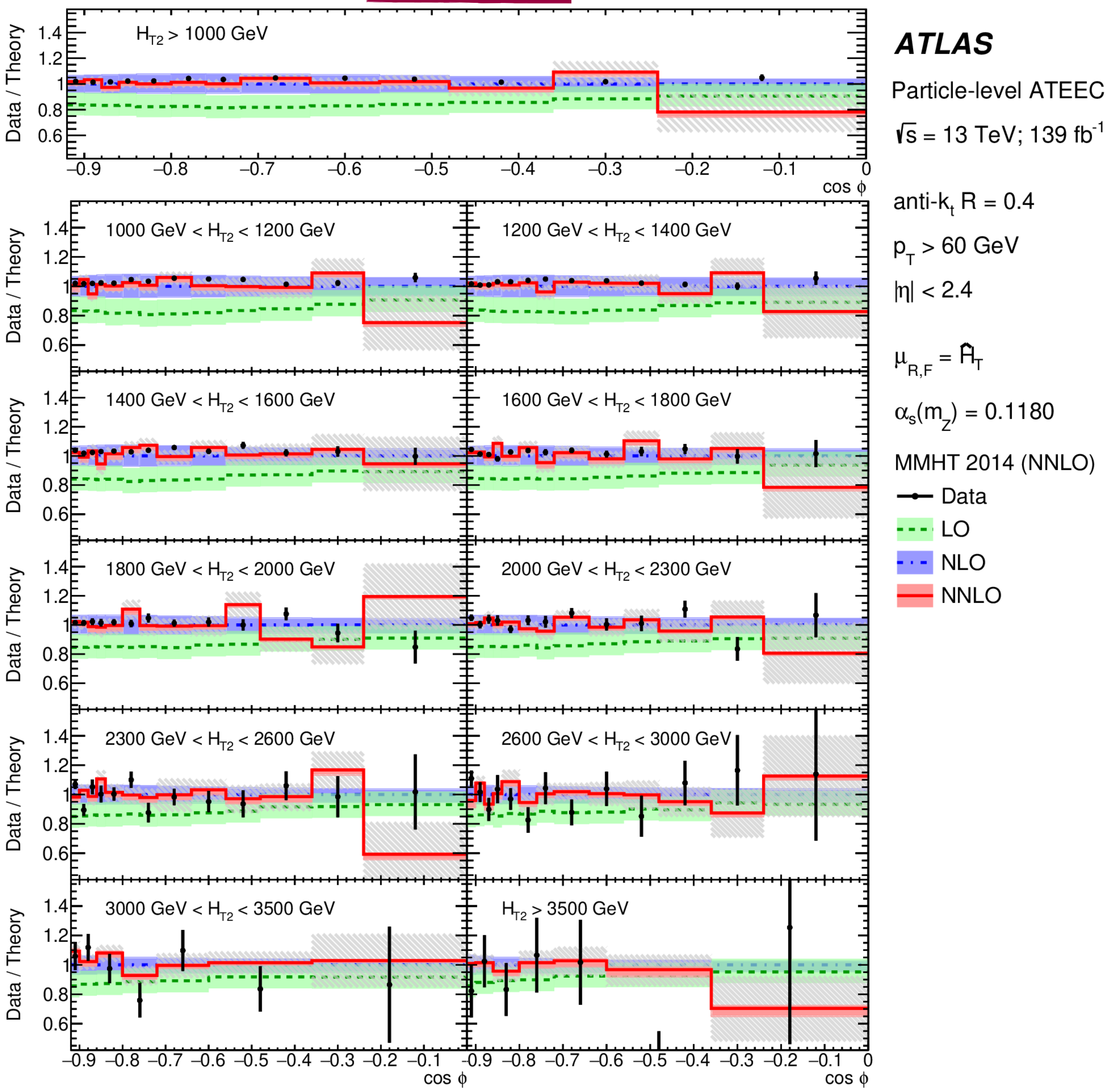

arXiv:2301.09351

- Excellent agreement between the data and theory with reduced theoretical uncertainties

Transverse energy-energy correlations: $\alpha_S(Q)$ determination

- Determination of $\alpha_S(Q)$ from the TEEC in 10 intervals at NNLO accuracy in pQCD, probing asymptotic freedom beyond the TeV scale
  - Values of $\alpha_S(m_Z)$ obtained for both the inclusive and 10 exclusive bins in H_{T2} using a χ^2 fit
  - The evolution of the $\alpha_S(m_Z)$ values from each of the exclusive fits leads to $\alpha_S(Q)$ values that are compared with the NNLO solution of the RGE
    - Scale choice: $Q = \hat{H}_T/2$
  - **Global fit results:**

TEEC: $\alpha_s(m_Z) = 0.1175 \pm 0.0006\ (\text{exp.})^{+0.0034}_{-0.0017}\ (\text{theo.})$

ATEEC: $\alpha_s(m_Z) = 0.1185 \pm 0.0009\ (\text{exp.})^{+0.0025}_{-0.0012}\ (\text{theo.})$

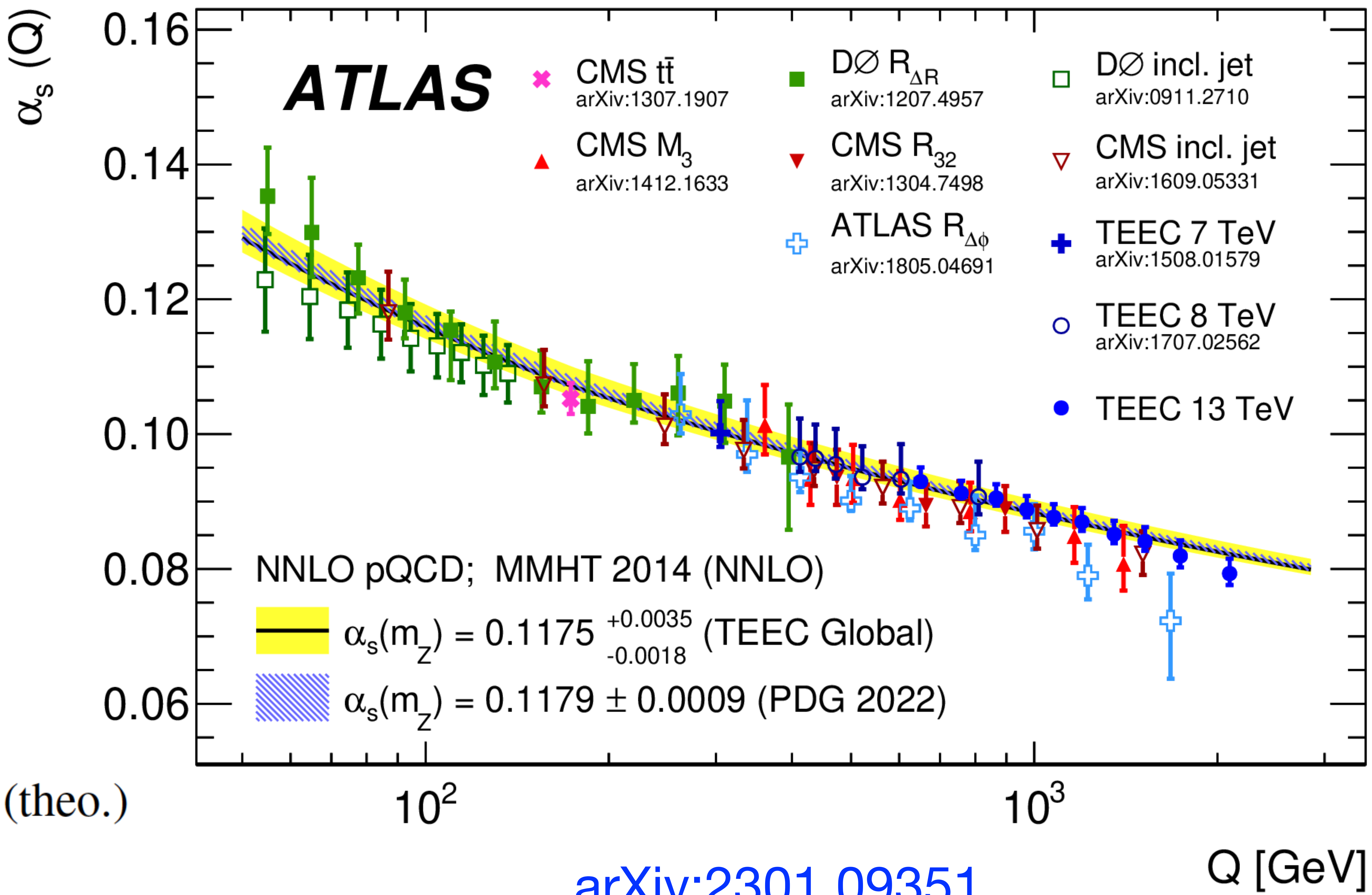

arXiv:2301.09351

Event isotropies using optimal transport: the Energy-Mover's Distance

- **Event isotropies** quantify how "far" a collider event $\mathscr{E}$ is from a symmetric radiation pattern $\mathscr{U}$, in terms of a Wasserstein distance metric

- **The Energy-Mover's Distance (EMD)** is defined as the minimum amount of "work" needed to transport one event $\mathscr{E}$ into another $\mathscr{E}'$ of equal energy, by a transportation plan f_{ij}, from particle i in one event, to particle j in another

$$\mathrm{EMD}_\beta(\mathscr{E}, \mathscr{E}') = \min_{\{f_{ij} \geq 0\}} \sum_{i=1}^{M} \sum_{j=1}^{M'} f_{ij}\, \theta_{ij}^{\beta},$$

θ_{ij}^{β}: ground measure between particles

This EMD uses a Wasserstein metric evaluated by solving the **Optimal Transport** problem

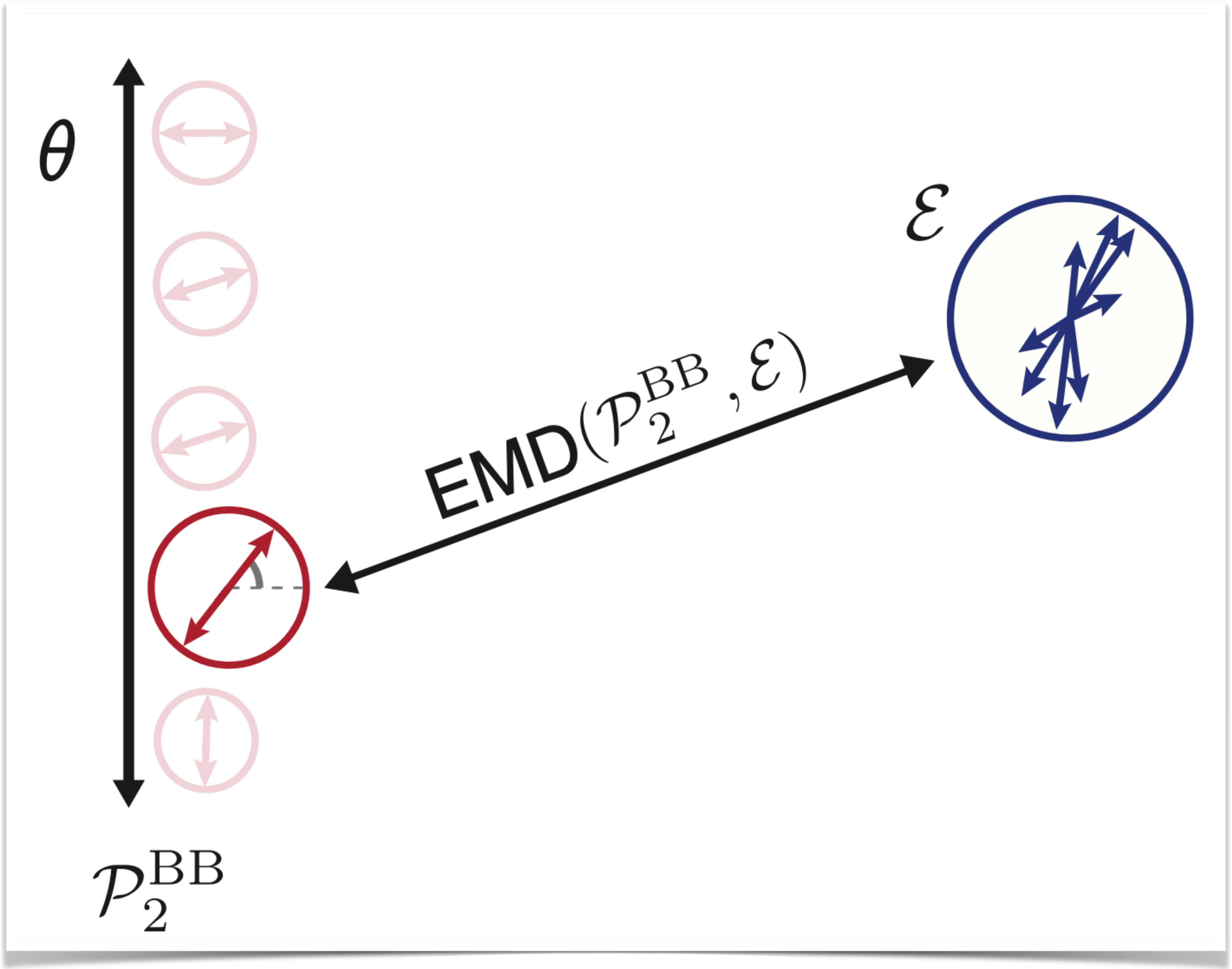

ATLAS-CONF-2022-056

- The event isotropies are defined as $I(\mathscr{E}) = \mathrm{EMD}(\mathscr{E}, \mathscr{U})$, bounded on $I(\mathscr{E}) \in [0,1]$ and infrared- and collinear- safe by construction

Event isotropies using optimal transport: measured observables

- **Three event shape observables are considered in this analysis:**

Geometry	Energy weight	Ground measure	Radiation pattern
Cylinder	$w_i^{\mathrm{Cyl}} = p_{\mathrm{T}i}/p_{\mathrm{T\,tot}}$	$\theta_{ij}^2 = \frac{12}{\pi^2 + 16y_{\max}^2}(y_{ij}^2 + \phi_{ij}^2)$	$\mathcal{U}_{16}^{\mathrm{Cyl}}$
Ring	$w_i^{\mathrm{Ring}} = p_{\mathrm{T}i}/p_{\mathrm{T\,tot}}$	$\theta_{ij}^2 = \frac{\pi}{\pi - 2}(1 - \cos\phi_{ij})$	$\mathcal{U}_{128}^{\mathrm{Ring}}$
Ring (dipole)	$w_i^{\mathrm{Ring}} = p_{\mathrm{T}i}/p_{\mathrm{T\,tot}}$	$\theta_{ij}^2 = \frac{1}{1 - 1/\sqrt{3}}(1 - \cos\phi_{ij})$	$\mathcal{U}_{2}^{\mathrm{Ring}}$

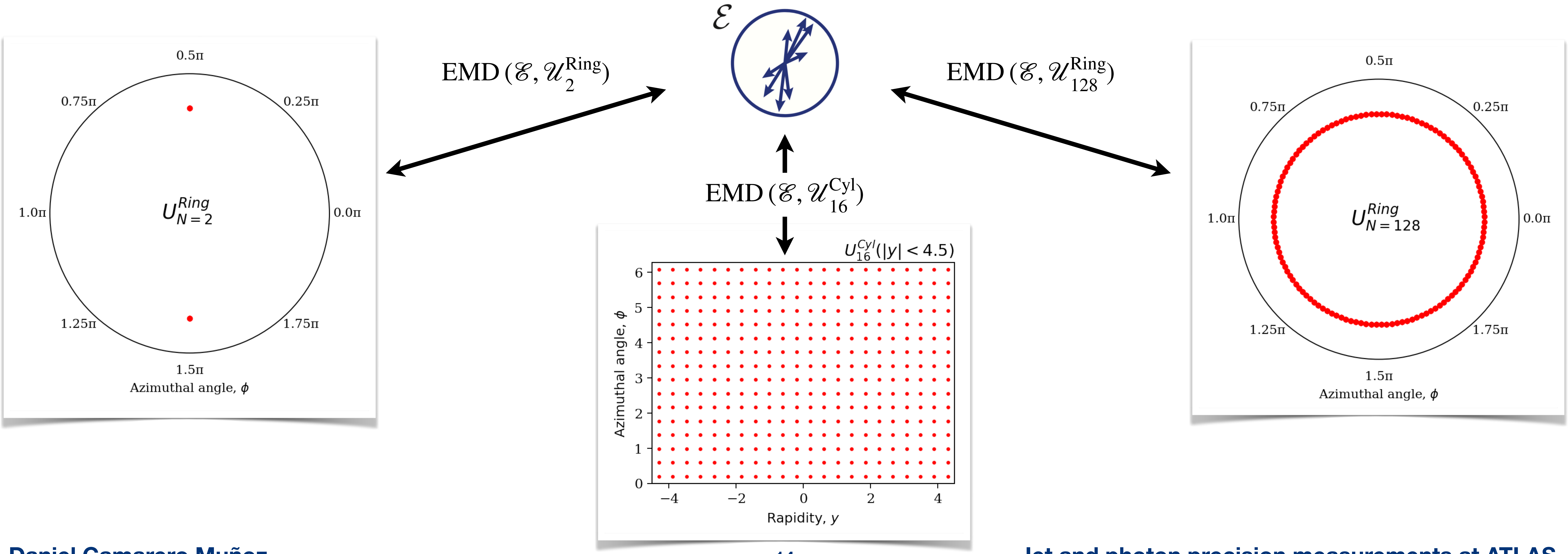

ATLAS-CONF-2022-056

Event isotropies using optimal transport: analysis methodology

- **Full Run-2 analysis performed using $139\ \mathrm{fb}^{-1}$**
  - Jet selection: $p_{\mathrm{T}} > 60\ \mathrm{GeV}$ and $|y| < 4.4$
  - Event selection: $N_{\mathrm{jet}} \geq 2$ and $H_{\mathrm{T2}} = p_{\mathrm{T1}} + p_{\mathrm{T2}} > 400\ \mathrm{GeV}$
  - Measurement performed in inclusive bins of: $N_{\mathrm{jet}} \geq 2$ to $N_{\mathrm{jet}} \geq 5$, $H_{\mathrm{T2}} > 500, 1000,$ and $1500\ \mathrm{GeV}$
- **Monte Carlo generators:**

Generator	Matrix element	PDF set	Parton shower	Hadronisation
PYTHIA	LO	NNPDF2.3 LO	p_{T}-ordered	Lund String
SHERPA (2 variants)	LO	CT14 NNLO	CS dipole	Cluster || Lund string
POWHEG + PYTHIA	NLO	NNPDF3.0 NLO	p_{T}-ordered	Lund String
POWHEG + HERWIG	NLO	NNPDF3.0 NLO	Angle-ordered	Cluster
HERWIG (2 variants)	NLO	MMHT2014 NLO	Angle-ordered || Dipole	Cluster

- **The main experimental uncertainties are:**
  - **MC modelling:** from the choice of MC to perform the unfolding. HERWIG angle-ordered vs PYTHIA.
  - **Jet energy scale and resolution:** the resolution dominates in almost all cases

Multi-jet event isotropies using optimal transport: $1 - I^{128}_{\text{Ring}}$ observable

Back-to-back ⟷ Isotropic

$$1 - I^{128}_{\text{Ring}} = 0.92$$

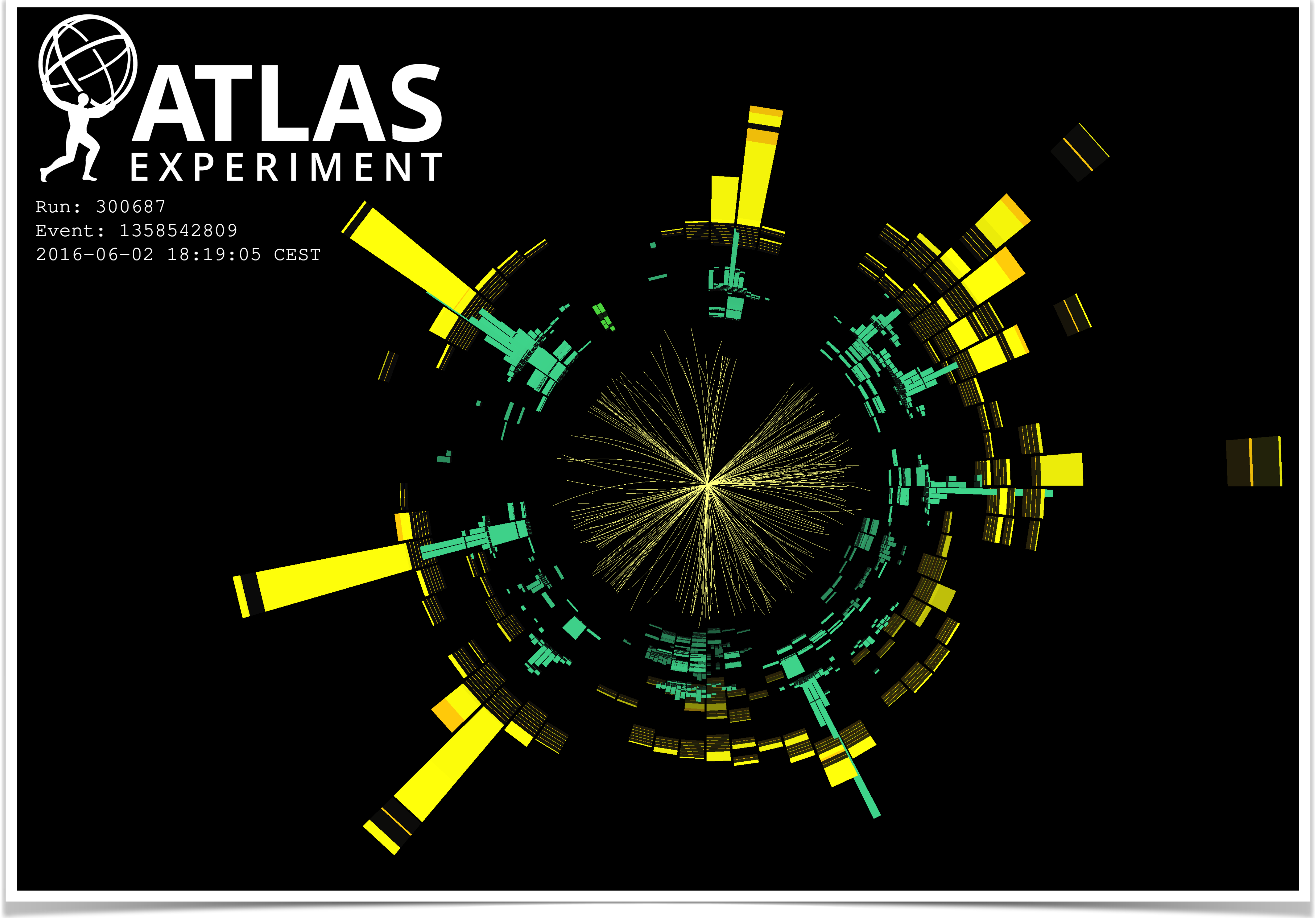

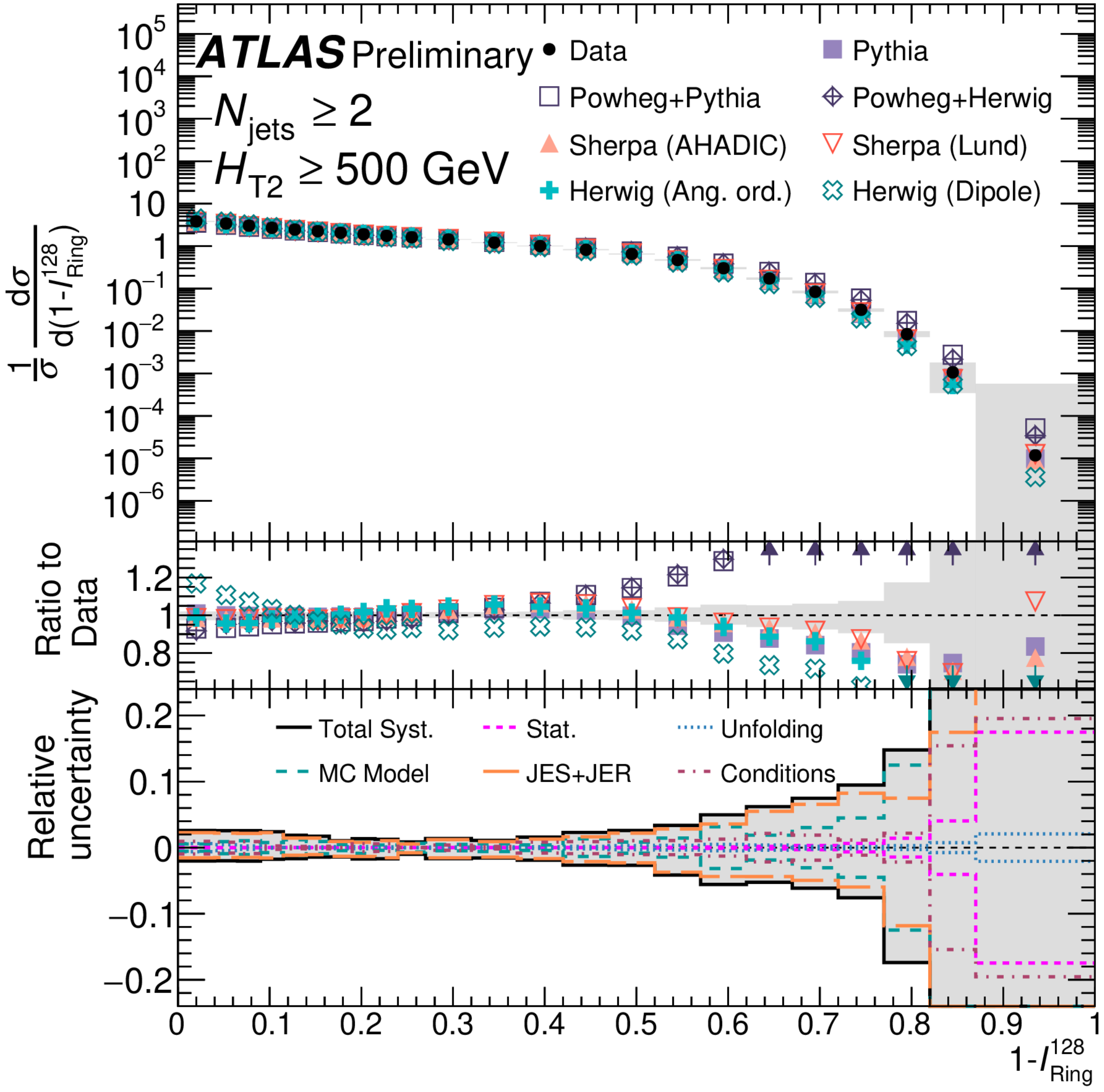

ATLAS-CONF-2022-056

Multi-jet event isotropies using optimal transport: $1 - I^{128}_{\mathrm{Ring}}$ observable

- **Ring-like event isotropy:**
  - Measurement of $1 - I^{128}_{\mathrm{Ring}}$ for $N_{\mathrm{jet}} \geq 2$ and $H_{\mathrm{T2}} > 500\ \mathrm{GeV}$
  - Distribution is saturated by well-balanced dijets events and by multijet events with isotropic configurations
  - Large dynamic range, as the cross section spans by ≈ 6 orders of magnitude
  - POWHEG predictions completely disagree with others
  - Large differences between HERWIG dipole vs angle-ordered
  - No notable differences between SHERPA hadronisation models

Back-to-back ⟷ Isotropic

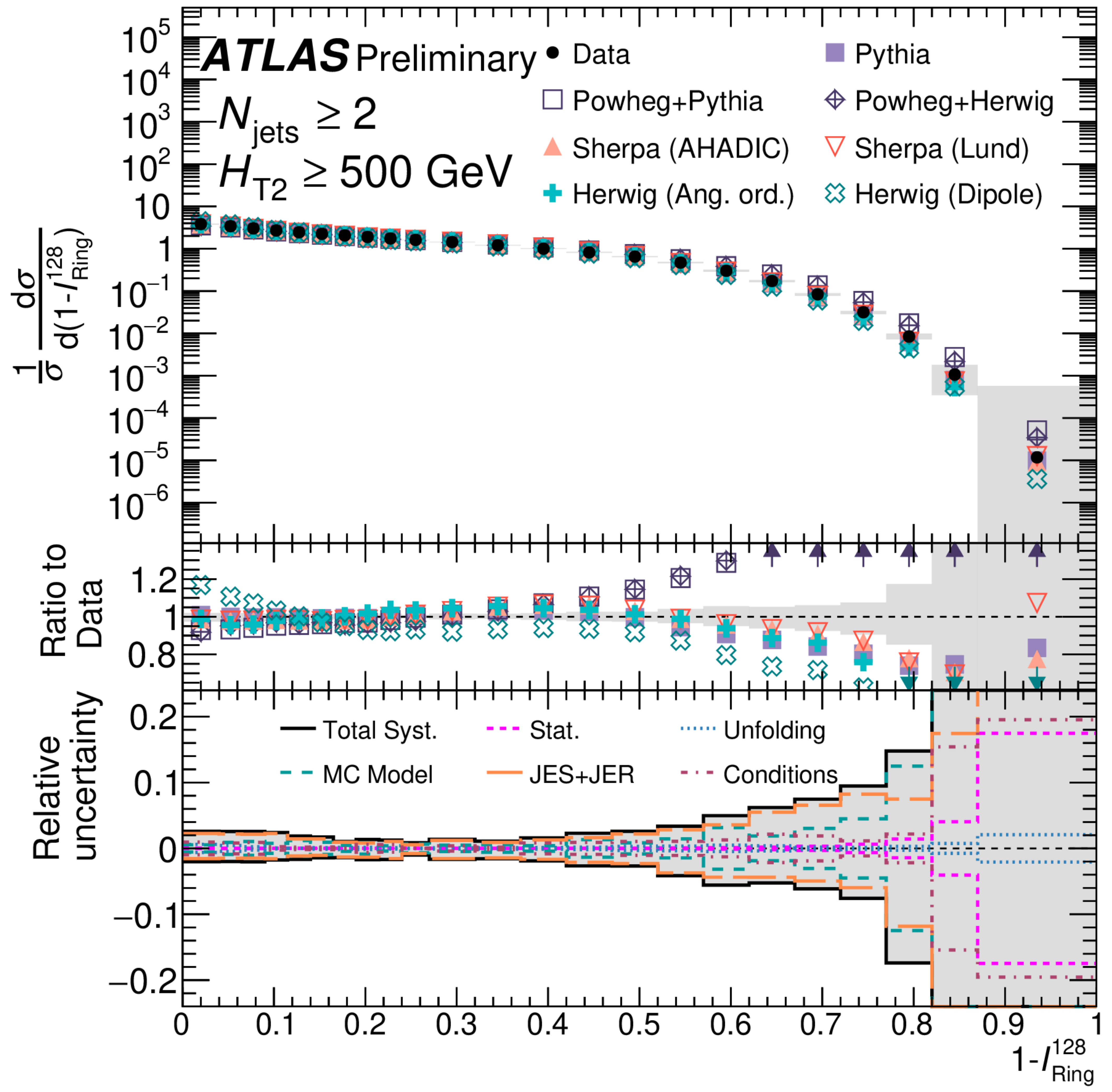

ATLAS-CONF-2022-056

Multi-jet event isotropies using optimal transport: $1 - I^{16}_{\mathrm{Cyl}}$ observable

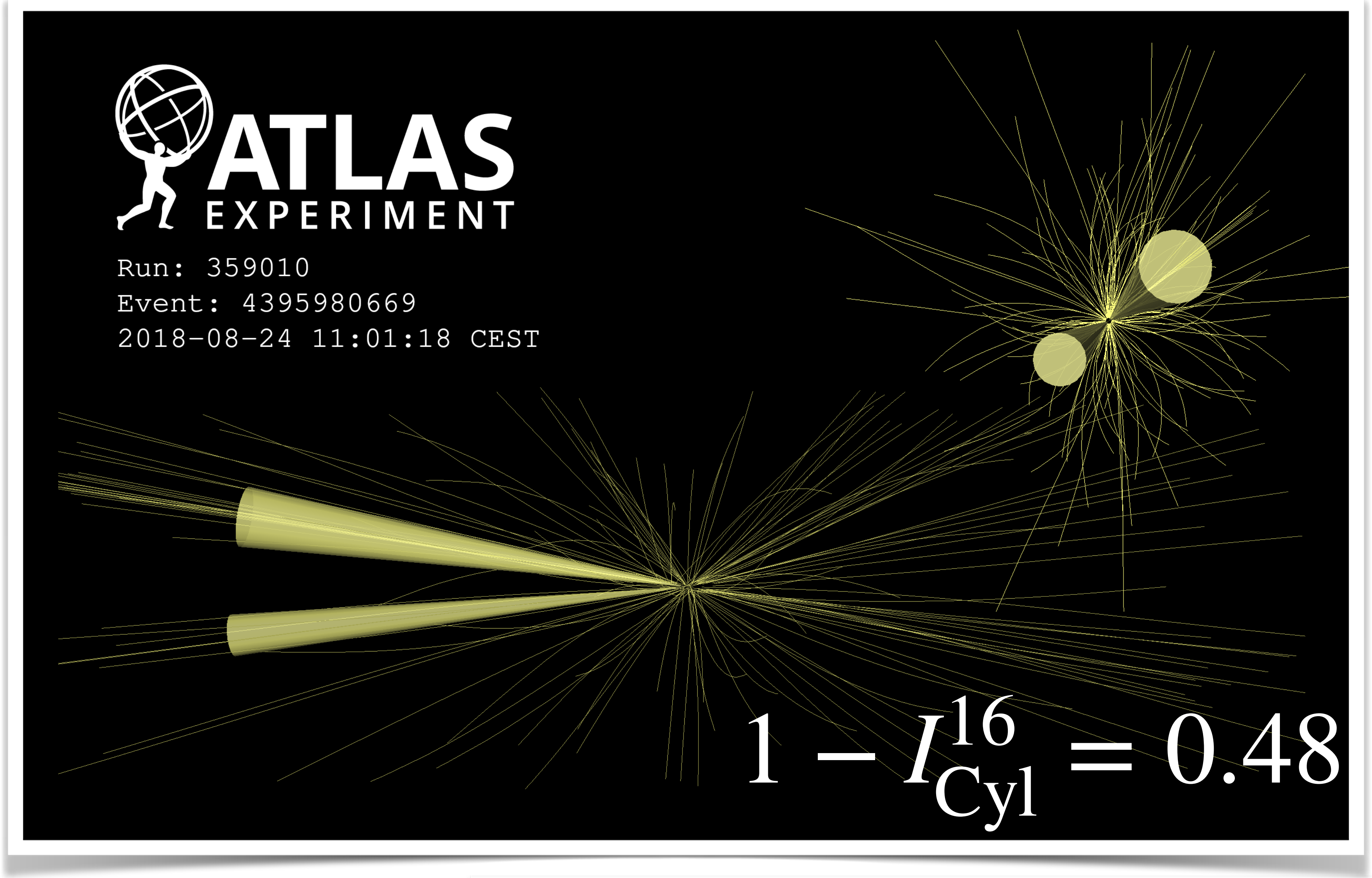

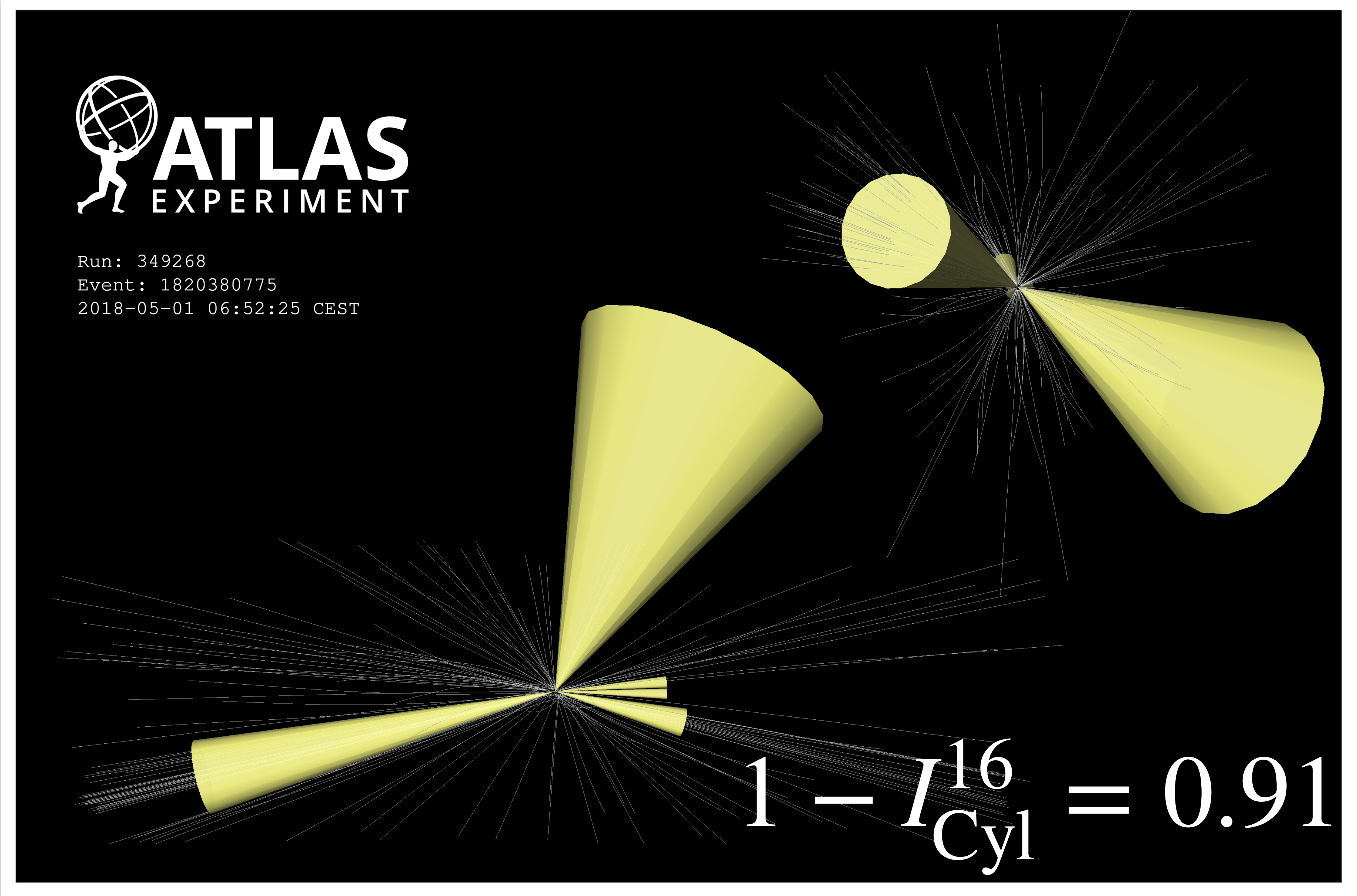

Non-isotropic ⟷ **Isotropic**

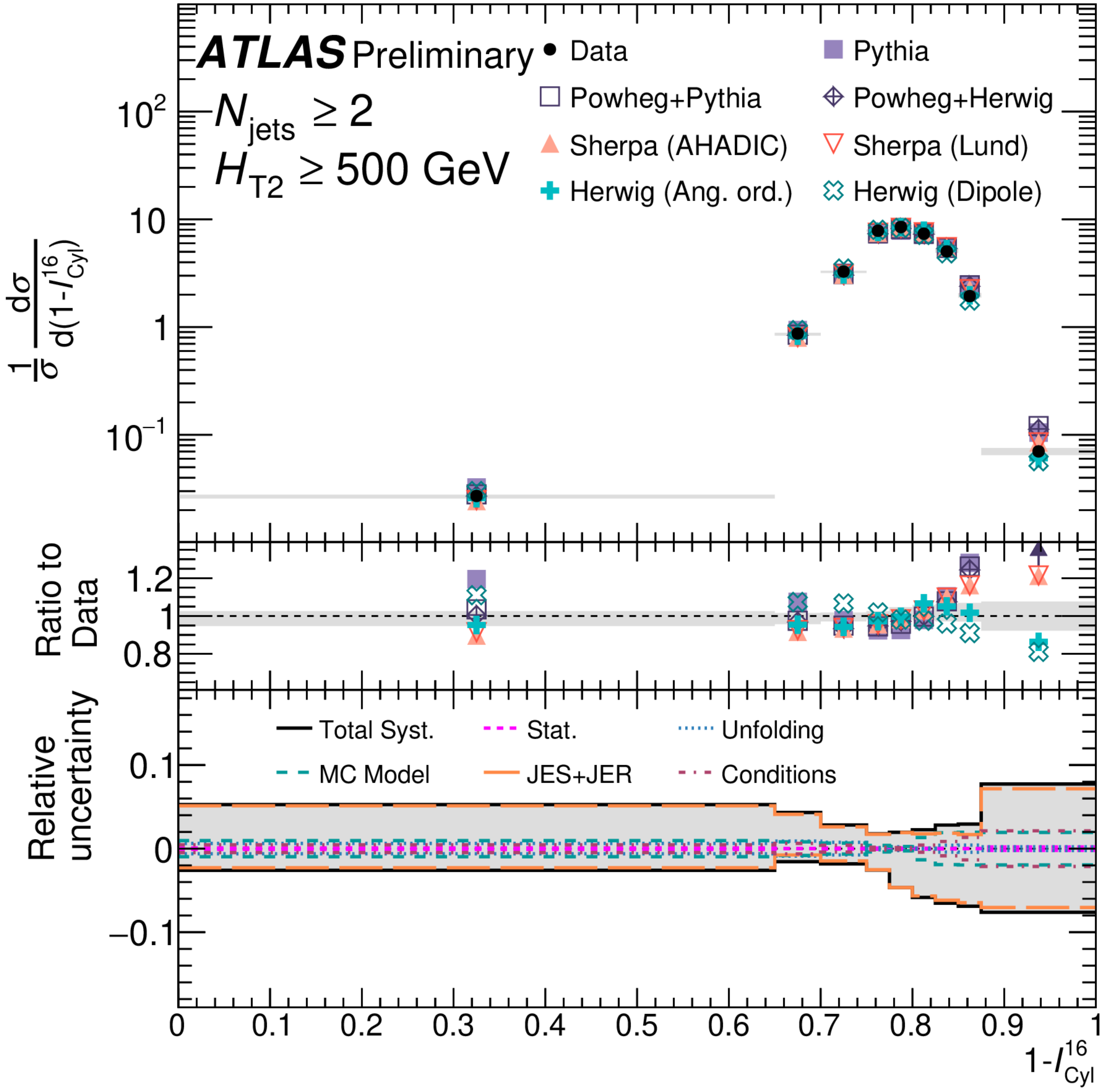

ATLAS-CONF-2022-056

Multi-jet event isotropies using optimal transport: $1 - I_{\text{Cyl}}^{16}$ observable

- **Cylindrical event isotropy:**
  - Measurement of $1 - I_{\text{Cyl}}^{16}$ for $N_{\text{jet}} \geq 2$ and $H_{\text{T2}} > 500$ GeV
  - Distribution is saturated by dijet events in the forward region of one side of the detector and by multijet events that evenly populate the rapidity-azimuth plane
  - None of the MC predictions accurately describe this observable
  - Different behaviour for different HERWIG parton shower models, PYTHIA and SHERPA predictions
  - PYTHIA and SHERPA differ in the tails
  - No sensitivity to hadronisation models

Non-isotropic ⟷ Isotropic

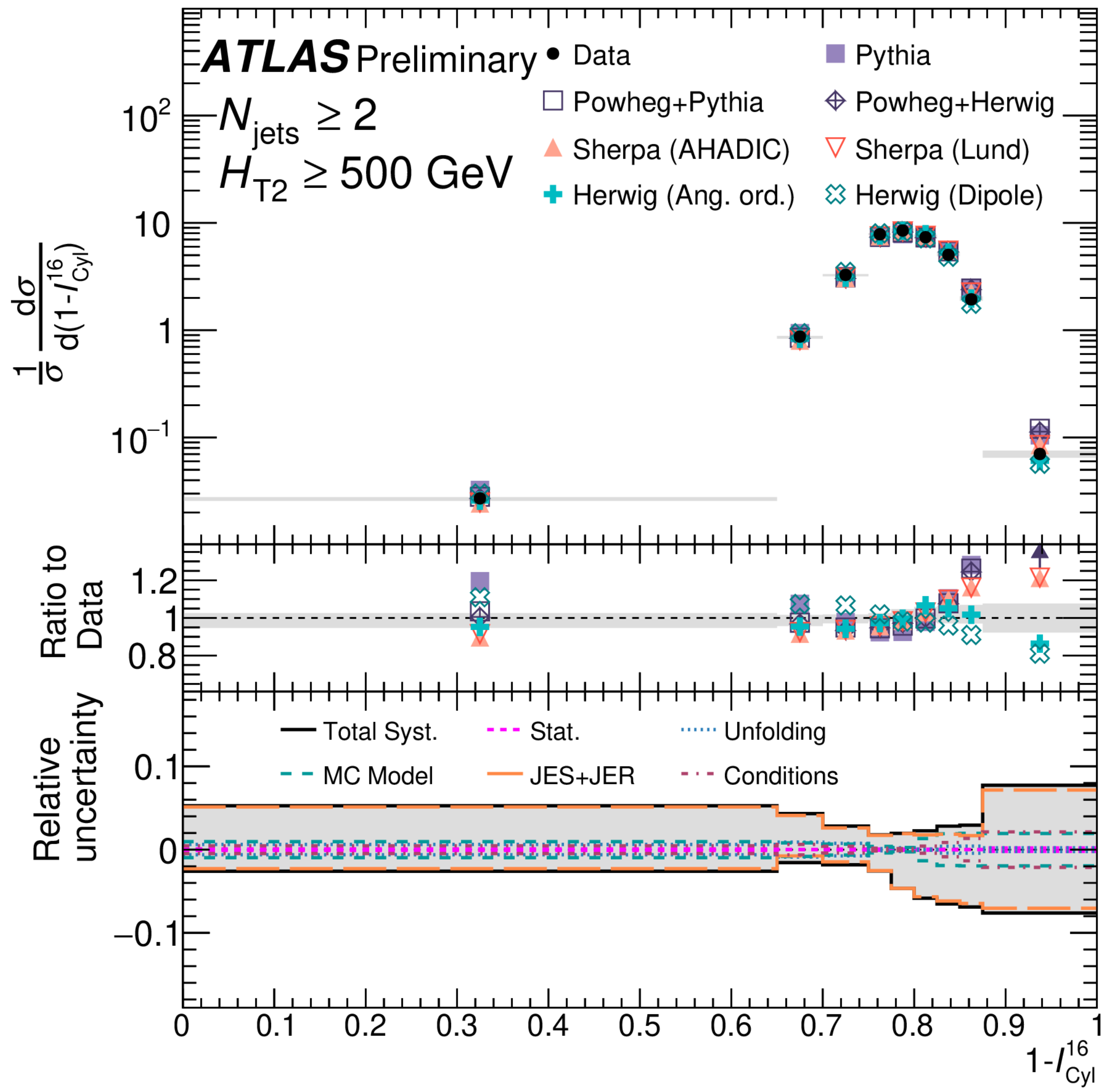

ATLAS-CONF-2022-056

Summary and conclusions

Three ATLAS measurements performed at $\sqrt{s} = 13\ \text{TeV}$ using $139\ \text{fb}^{-1}$ have been presented

Inclusive-photon production and its dependence on photon isolation:

- The dependence on R of the measured cross sections, measured for first time, is well described by NLO JETPHOX and NNLO NNLOJET pQCD predictions
  - Validation of the underlying pQCD theoretical description up to $\mathcal{O}(\alpha_S^2)$

Determination of the strong coupling constant from TEEC

- Theoretical uncertainties reduced by a factor of 3 thanks to the inclusion of NNLO corrections
  - The evolved $\alpha_S(Q)$ values are compared with the NNLO solution of the RGE showing good agreement up to the highest energy scales and with previous measurements

Multi-jet event isotropies using optimal transport:

- First application of optimal transport techniques in a collider physics measurement
  - Agreement between unfolded data and simulations tends to be best in balanced dijet-like arrangements and deteriorates in more isotropic configurations

Back-up

Inclusive-photon production: systematic uncertainties

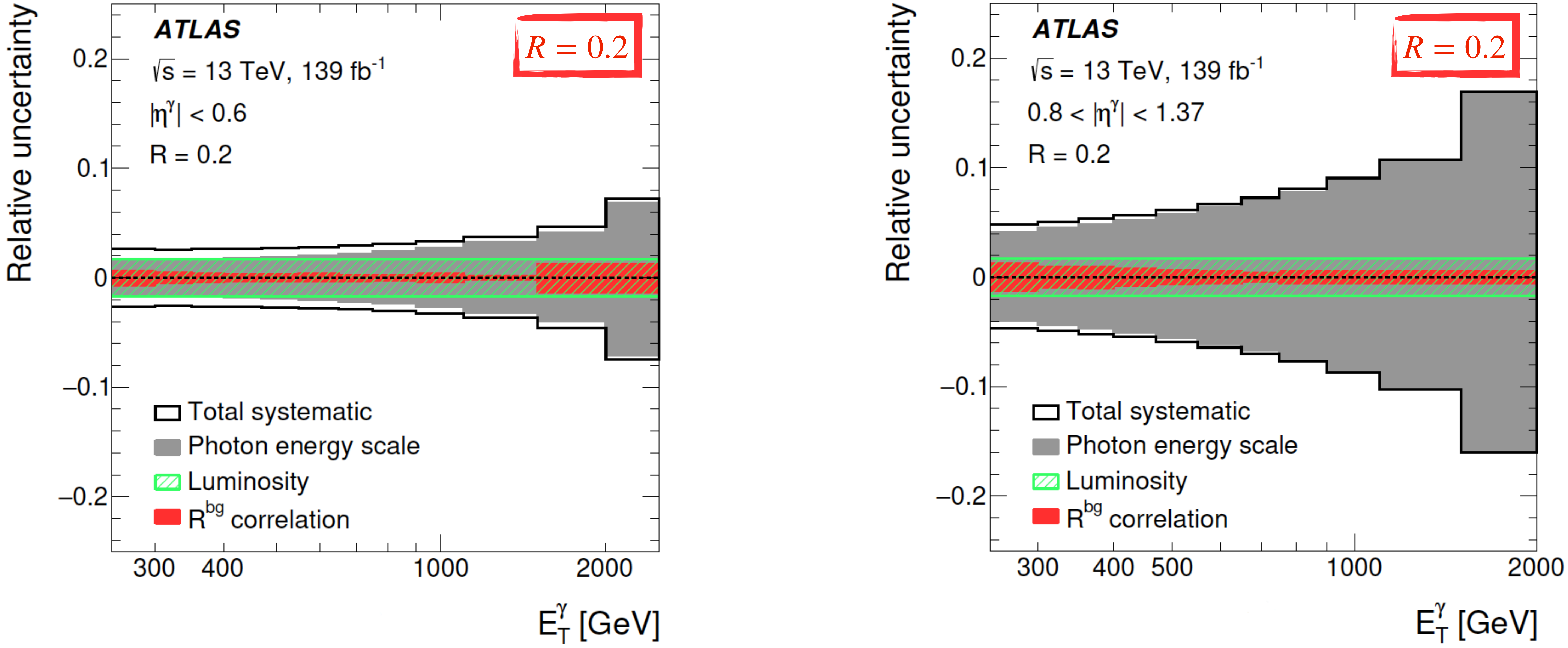

arXiv:2302.00510

- Uncertainty due to the photon energy scale is dominant: $2\% - 17\,\%$ ($3\% - 20\,\%$) reached for $|\eta^\gamma| < 1.37$ ($|\eta^\gamma| > 1.56$)
- The uncertainty due to the luminosity ($1.7\,\%$) dominates at low E_T^γ
- The uncertainty due to the $R^{\rm bg}$ correlation is important at low and medium E_T^γ: $0.5\% - 2\,\%$

Inclusive-photon production: systematic uncertainties

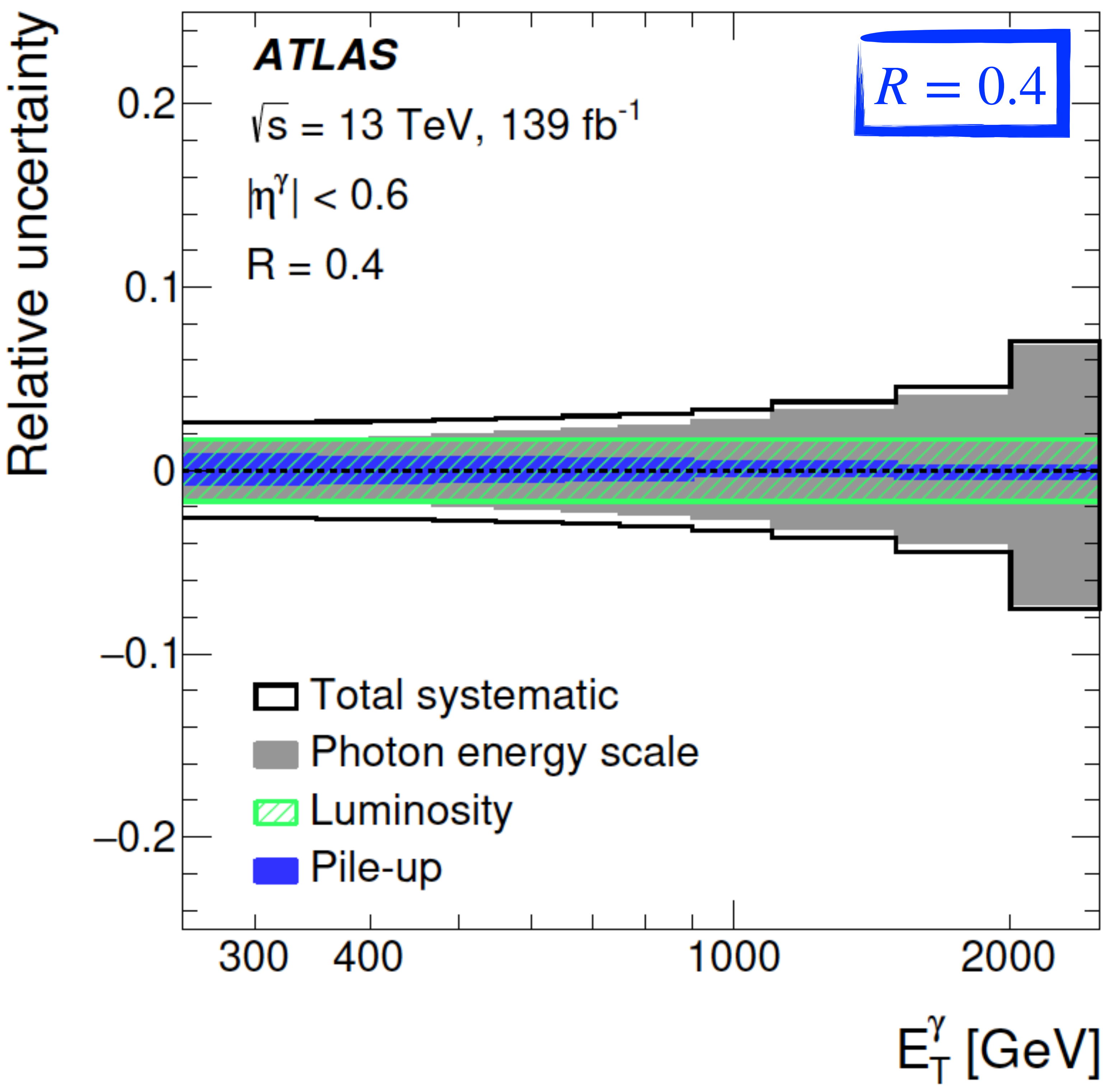

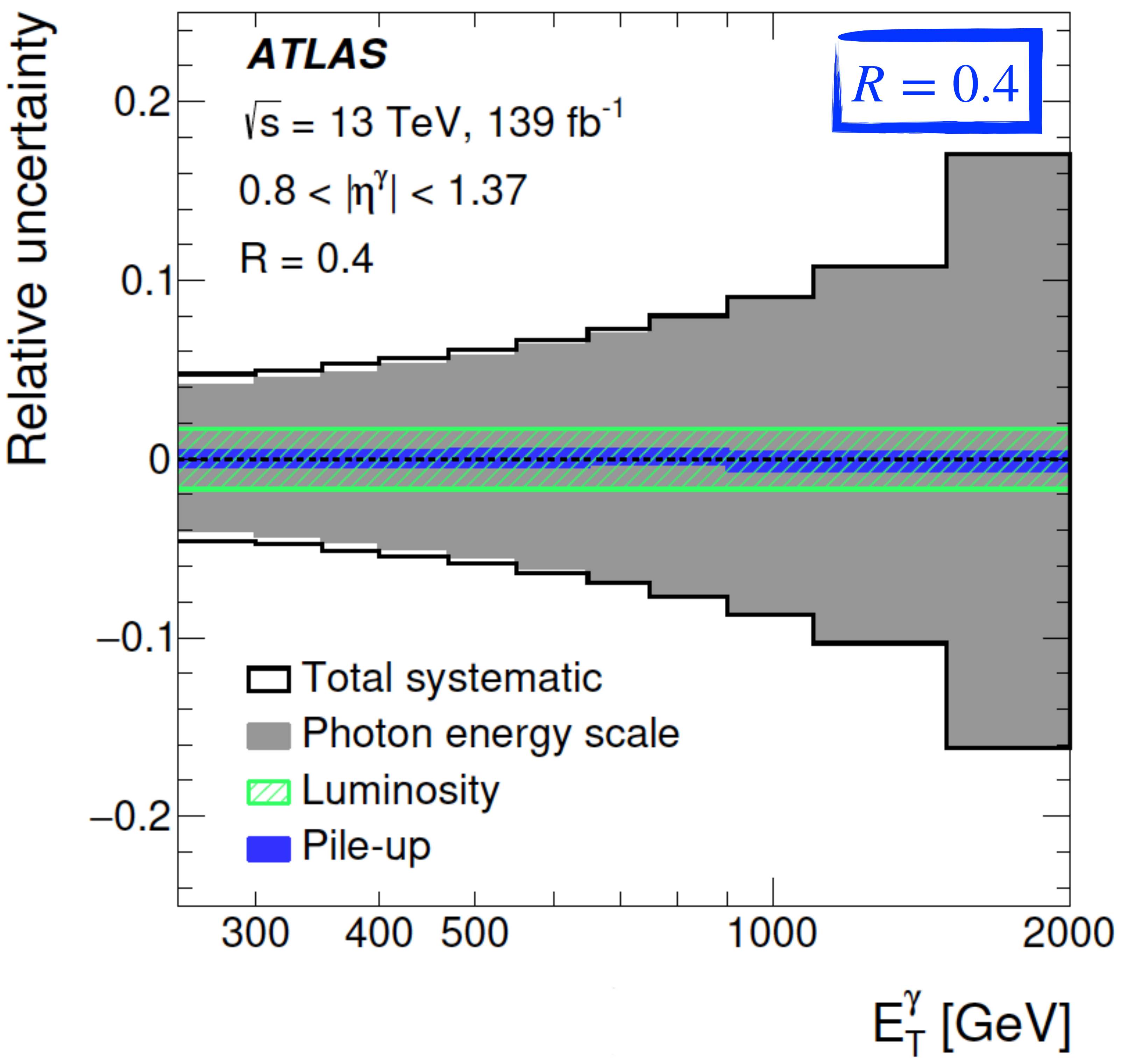

arXiv:2302.00510

- Uncertainty due to the photon energy scale is dominant: $2\% - 17\,\%$ ($3\% - 20\,\%$) reached for $|\eta^{\gamma}| < 1.37$ ($|\eta^{\gamma}| > 1.56$)
- The uncertainty due to the luminosity ($1.7\,\%$) dominates at low E_T^{γ}
- The uncertainty due to the pile-up is important at low and medium E_T^{γ}: $0.5\% - 1.5\,\%$

Transverse energy-energy correlations: $\alpha_S(m_Z)$ values

- Comparison of the values of $\alpha_S(m_Z)$ determined from different analyses by ATLAS and CMS